Cyclotron wave spectrum in bismuth and observation of the spectral boundaries in a nonlinear microwave experiment

M. R. Trunin

Institute of Solid State Physics, Academy of Sciences of the USSR
(Submitted 21 November 1984)
Zh. Eksp. Teor. Fiz. **88**, 1834–1846 (May 1985)

Results are given of a numerical solution of the dispersion equation for cyclotron waves in Bi in the electron cyclotron resonance region. The case of wave propagation along the C_3 axis in a magnetic field $\mathbf{H}\|C_1$ is considered. An ellipsoidal model of the Bi Fermi surface is employed in the calculations. It is shown that, in the intermediate wavelength region ($kR \gg 1$, where R is the cyclotron radius) the frequency is an oscillatory function of the wave vector k. Asymptotic formulas are presented that describe the behavior of the wave dispersion law for $kR \gg 1$ with a high degree of accuracy. Comparison of experimental data with the calculations suggests that the properties of a nonlinear signal that is reflected from the bismuth sample surface can be interpreted as being due to the boundary of the longitudinal cyclotron wave spectrum.

INTRODUCTION

In metals near cyclotron resonances cyclotron waves are found which propagate perpendicularly to the external magnetic field ($\mathbf{k}\perp\mathbf{H}$). Depending on the relative orientation of the electric field $\mathbf{E}$ and the external field $\mathbf{H}$ of the wave, we distinguish ordinary ($\mathbf{E}\|\mathbf{H}$) and extraordinary ($\mathbf{E}\perp\mathbf{H}$) cyclotron waves. Theoretical investigations of the properties of cyclotron waves have shown that in metals with a spherical Fermi surface, both short ($kR \gg 1$) and long ($kR \ll 1$) cyclotron waves can be excited (here R is the Larmor radius).

In the limiting case $kR \gg 1$, which is considered in Ref. 1, the extraordinary mode splits into longitudinal ($\mathbf{E}\|\mathbf{k}$, $\mathbf{E}\perp\mathbf{H}$) and transverse ($\mathbf{E}\perp\mathbf{k}$, $\mathbf{E}\perp\mathbf{H}$) modes. The ordinary wave ($\mathbf{E}\perp\mathbf{k}$, $\mathbf{E}\|\mathbf{H}$) is transverse. All three waves are linearly polarized. The spectra of the transverse waves exhibit normal dispersion (the frequency increases as a function of k) and approach the cyclotron resonance line from the high-magnetic-field side. The longitudinal wave spectrum exhibits anomalous dispersion and is localized close to the cyclotron resonance on the low-field side.

In the other limiting case $kR \ll 1$, which is considered in Ref. 2, the ordinary wave is linearly polarized while the extraordinary wave is elliptically polarized in a plane perpendicular to the magnetic field. Both waves exhibit anomalous dispersion and lie near the cyclotron resonance line on the high-magnetic-field side. In the intermediate case $kR \gtrsim 1$, in a spherical model for the ordinary and extraordinary waves, the frequency is observed to be an oscillatory function of the wave vector.

The waves that are most accessible to observation are those in the region of weak spatial dispersion $kR \ll 1$. Their wavelengths are comparable with the thicknes of the sample, and as the field H changes the surface resistance of the metal $\zeta(H)$ experiences oscillations, brought about by the excitation of standing waves. The long-wavelength cyclotron waves were studied experimentally in alkali metals[2,5] and in bismuth, near electron[6–8] and hole[9] cyclotron resonances. The features associated with the oscillatory character of the dispersion curve at $kR \gtrsim 1$ were observed only in silver[10] and

potassium.[11]

In the present work, we present the results of a numerical solution of the dispersion equation of cyclotron waves in Bi in the geometry $\mathbf{H}\|C_1$, $\mathbf{k}\|C_3$. The region of the first cyclotron resonance of electrons having large mass is considered in detail. An experiment is discussed in which nonlinear reflected signals from the surface of a Bi sample (at the frequency of the second harmonic) are recorded as a function of the external field H. The location of the features observed in this experiment at certain values of the field H are identical with the boundaries of the spectrum of longitudinal cyclotron waves in Bi.

THEORY

Let an electromagnetic wave of frequency be incident normally on a sample of bismuth placed in a constant magnetic field $\mathbf{H}$ parallel to its surface. We choose a rectangular xyz system of coordinates in which the z axis is directed along $\mathbf{H}$ and the y axis coincides with the normal to the surface of the sample. The propagation of the electromagnetic wave in the unbounded metal is described by Maxwell's equations, in which we can neglect the displacement current for $\omega \ll \omega_0$, where ω_0 is the plasma frequency. After elimination of the variable magnetic field and the longitudinal component of the electric field, Maxwell's equations, written in the Fourier representation, lead to a set of linear homogeneous equations for the transverse components of the electric field. Setting the determinant of this system equal to zero, we obtain the dispersion equation of the propagating waves:

$$\begin{vmatrix} k^2 - \dfrac{4\pi i\omega}{c^2}\left(\sigma_{xx} - \dfrac{\sigma_{xy}\sigma_{yx}}{\sigma_{yy}}\right) & \dfrac{4\pi i\omega}{c^2}\left(\sigma_{xz} - \dfrac{\sigma_{xy}\sigma_{yz}}{\sigma_{yy}}\right) \\[2ex] \dfrac{4\pi i\omega}{c^2}\left(\sigma_{zx} - \dfrac{\sigma_{yx}\sigma_{zy}}{\sigma_{yy}}\right) & k^2 - \dfrac{4\pi i\omega}{c^2}\left(\sigma_{zz} - \dfrac{\sigma_{yz}\sigma_{zy}}{\sigma_{yy}}\right) \end{vmatrix} = 0,$$

$$(1)$$

where $\sigma_{ij}(k,\omega)$ are the Fourier components of the conductivity tensor. In the field H, the expression for the elements of the tensor σ_{ij}, for an arbitrary carrier dispersion law, has the following form:

$$\sigma_{ij} = \frac{4\pi e^2}{(2\pi\hbar)^3} \sum_{n=-\infty}^{\infty} \sum \int_{-p_{z\,max}}^{p_{z\,max}} dp_z \frac{mv_{in}^* v_{jn}}{\nu - i(\omega - n\Omega)}, \qquad (2)$$

where

$$v_{jn} = \frac{1}{2\pi} \int_0^{2\pi} d\varphi\, v_j(\varphi) \exp\left[\frac{i}{\Omega}\int_0^\varphi d\varphi'\,(kv_y) - in\varphi\right]. \qquad (3)$$

Here v_j is the component of the velocity vector on the Fermi surface, p_z is the projection of the momentum on the z axis, φ is the phase of the periodic motion along the trajectory in the constant magnetic field, and ν is the collision frequency. The first sum in (2) corresponds to summation over all types of carriers.

The Fermi surface of bismuth consists of three electron surfaces and one hole surface, very similar in shape to ellipsoidal. In Appendix A, we calculate the components of the conductivity tensor for an ellipsoid oriented arbitrarily with respect to the x, y, z axes.

We now consider the case $\mathbf{H}\|C_1\|z$, $\mathbf{k}\|C_3\|y$, $C_2\|x$. The electron ellipsoids of bismuth are quite extended and are inclined to the trigonal plane at an angle of about 6°. The energy of the electrons of one of the ellipsoids can be represented in the form

$$\varepsilon_a(p) = \frac{1}{2m_0}(\alpha_1 p_x^2 + \alpha_2 p_y^2 + \alpha_3 p_z^2 + 2\alpha_4 p_y p_z), \qquad (4)$$

where p_x, p_y, p_z are the components of the momentum vector along the binary C_2, the trigonal C_3 and the bisector C_1 axes, and m_0 is the mass of a free electron. The values of the elements of the reciprocal mass tensor and the Fermi surface of the electrons are taken from Ref. 13:

$$\alpha_1 = 166.7; \quad \alpha_2 = 89.5; \quad \alpha_3 = 1.8;$$
$$\alpha_4 = 9.4; \quad \varepsilon = 2.75 \cdot 10^{-14}\ \text{erg}.$$

The ellipsoid (4) we call ellipsoid (a). The dispersion law of the other two ellipsoids (b) and (c) is obtained by rotating ellipsoid (a) by 120° around the trigonal axis. The hole zone of bismuth represents an ellipsoid of rotation (d) around the trigonal axis. The energy of the hole is

$$\varepsilon_d(p) = p_x^2/2M_1 + p_y^2/2M_3 + p_z^2/2M_1, \qquad (5)$$

where, according to Ref. 14, $M_1 = 0.063 m_0$; $M_3 = 0.65 m_0$; $\varepsilon_d = 1.875 \times 10^{-14}$ erg.

The use of the Fermi surface parameters given above leads to excellent quantitative agreement of the experimental and calculated spectra of the long-wavelength cyclotron waves in Bi.[8,9] In this geometry, the cyclotron masses of the electrons of ellipsoids (b) and (c) are equal, and are twice the mass of the electrons of ellipsoid (a):

$$m^{(b)} = m^{(c)} = 2m_0(\alpha_1\alpha_2 + 3\alpha_2\alpha_3 - 3\alpha_4^2)^{-1/2} \approx 2m^{(a)} = 2m_0(\alpha_1\alpha_2)^{-1/2}. \qquad (6)$$

The cyclotron mass of the holes is much greater than the cyclotron mass of the electrons:

$$m^{(d)} = (M_1 M_3)^{1/2} = 12.45 m^{(b)}. \qquad (7)$$

We are interested in the spectrum of the cyclotron wave in magnetic fields that are larger than the field of the first order cyclotron resonance of the electrons of ellipsoids (b) and (c). In what follows, the indices (b) and (c), which indicate

equal electron masses, radii and frequencies for these electrons, will be omitted.

In the general case, to determine the dependence of kR on Ω/ω it is necessary to solve the complicated dispersion equation (1), in which the elements of the conductivity tensor are obtained as a result of calculating the σ_{ij} components for each species of carriers in Bi according to formulas (A4) and (A5) of Appendix A and subsequently summarizing the contributions from the different species. In the absence of collisions ($\Omega/\nu \to \infty$), for arbitrary kR, the wave spectrum was calculated numerically directly from the general equation (1). In expression (A5), we took into account the first fifteen terms of the sum ($n_{max} = 15$), and the Bessel functions and their integrals were calculated to an accuracy of 10^{-3}. The result of the calculation of the cyclotron wave spectrum in the interval $0 \leqslant kT \leqslant 8$, $1 \leqslant \Omega/\omega \leqslant 2.5$ are shown in Fig. 1. We emphasize that the dependence of kR on Ω/ω is obtained for the frequency $\omega/2\pi = 9.3$ GHz. We consider the origin of the different branches of the spectrum of the cyclotron waves in limiting cases of weak and strong spatial dispersion.

In the long-wavelength region ($kR \ll 1$), the expressions for the elements of the conductivity tensor are easily replaced by their asymptotic expansions. To within terms of order $(kR)^2$, the non-Hall off-diagonal terms are small in comparison with the remaining elements of the conductivity tensor. In this approximation, the dispersion equation (1) breaks up into a system of two equations which are analogous to the equations that determine the propagation of ordinary and extraordinary cyclotron waves in the case of a spherical Fermi surface.[5] In Bi, for the $\mathbf{H}\|C_1$, $\mathbf{k}\|C_3$ geometry we are considering, for both types of waves, the quantity kR increases monotonically as the magnetic field decreases, so that, near resonance, waves with small values of k do not exist. In the ordinary wave case (the o branch in Fig. 1) a region $1.5 < \Omega/\omega \leqslant 2.32$ exists sufficiently close to resonance, in which $0 \leqslant kR < 1$ and use of the approximation $kR \ll 1$ is valid. For the extraordinary wave, there is no such region in this interval $1 < \Omega/\omega < 2.5$, and we can only note that the branch b in Fig. 1 is a continuation of the dispersion curve of the wave with $\mathbf{E}\perp\mathbf{H}$, $\mathbf{E}\perp\mathbf{k}$, described by Eq. (9) in the case $kR \gg 1$ (see below).

In the short-wavelength region ($kR > 1$), the spectrum
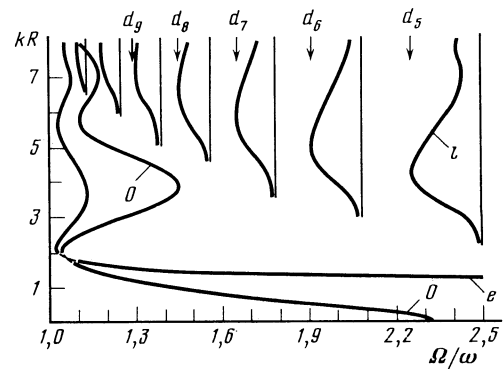
FIG. 1. Spectrum of cyclotron waves in Bi in the region of the first electron cyclotron resonance, obtained on the basis of a solution of the general dispersion equation (1); $\mathbf{H}\|C_1$, $\mathbf{k}\|C_3$, $\omega/2\pi = 9.3$ GHz, $\Omega/\nu \to \infty$.

shown in Fig. 1 contains two oscillatory branches, squeezed toward the right side of the $\Omega/\omega = 1$ line with increasing k, and also branches, lying to the left of the high-order hole resonances. In accord with (7), the hole resonances of orders $5 \leqslant n \leqslant 12$ are located in the interval $1 < \Omega/\omega < 2.5$. Their location coincides with the vertical cuts on Fig. 1 (the $n = 12$ resonance is not oberved).

In the case $kR \gg 1$, as follows from Appendix B, where the asymptotic expressions are calculated for the components σ_{ij}, the dispersion equation (1) decomposes into three equations that determine the propagation of linearly polarized waves:

$$k^2 - (4\pi i\omega/c^2)\sigma_{zz} = 0, \tag{8}$$

$$k^2 - (4\pi i\omega/c^2)\sigma_{xx} = 0, \tag{9}$$

$$\sigma_{yy} = 0. \tag{10}$$

The solutions of Eqs. (8) and (9), which are found with the use of the approximate expressions (B7) and (B8), determine the oscillatory spectrum of the transverse waves. At $kR > 8$, the dispersion curves rapidly approach the cyclotron resonance line $\Omega/\omega = 1$. Comparing Fig. 1 with the spectrum calculated from (8) and (9), it is easy to see that the oscillatory branch at the right in Fig. 1 corresponds to the ordinary wave (8), while the one on the left is determined by the solution of Eq. (9). The accuracy of the asymptotic calculation is equal to 1.5% in Ω/ω at $kR = 8$. At $kR = 3.9$, the solution of the general equation (1) determines the turning point $(\Omega/\omega)_0 = 1.45$ (Fig. 1), while at $kR = 3.9$, the solution (8) with, the help of (B7) and (B8), gives the value $(\Omega/\omega)_0 = 1.40$ for the boundary of the spectrum of the ordinary wave.

The branches associated with the hole resonances on Fig. 1 are described by Eq. (10). The existence of the longitudinal wave in magnetic fields greater than the field of the first resonance of the ellipsoid (b) electrons is governed by the presence in Bi of the hole ellipsoid (in the model of a spherical Fermi surface in this range of fields, Eq. (10) has no solutions). In Fig. 1, we denote the turning points of the longitudinal wave spectrum by the symbol d_i near the corresponding orders of the hole resonances; we have, in units of Ω/ω, $d_5 = 2.24$; $d_6 = 1.91$; $d_7 = 1.65$; $d_8 = 1.46$; $d_9 = 1.30$.

As an example of an oscillating solution of Eq. (10) we show the spectrum of the longitudinal wave (Fig. 2) in the region of the first hole resonance, where the oscillations are more clearly expressed. The dashed curve corresponds to the numerical solution of the general equation (1).

The physical reason for the appearance of oscillations in Fig. 1 and 2 is analogous to the origin of oscillations of the ultrasonic absorption coefficient in metals.[15] The electron interacts most effectively with the field of short waves at those portions of the trajectory in which it is moving almost parallel to the plane at constant wave phase. If an even number of half waves is included in the diameter of the orbit, then the absorption of the energy of the wave by the electron will be minimal. Consequently, in a fixed magnetic field, propagation of the wave is found to be possible at points kR differing by π. Actually, as follows from Fig. 1 and 2, in the region
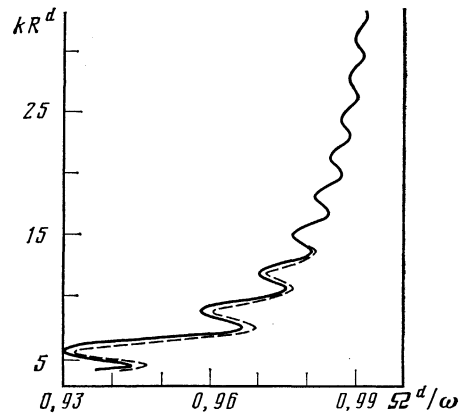
FIG. 2. Dispersion curve of a longitudinal cyclotron wave in Bi near the first hole cyclotron resonance. $\mathbf{H} \| C_1$, $\mathbf{k} \| C_3$. The solid curve is the solution of Eq. (10); the dashed curve is the solution of the general equation (1).

$kR \gg 1$, near the first-order electron and hole cyclotron resonances, the dependences of kR on (Ω/ω) are described by oscillating curves, while the period of the oscillation of kR is approximately π.

COMPARISON WITH EXPERIMENT

The waves are usually observed as follows. A metal plate is placed in an external magnetic field $\mathbf{H}$ and is irradiated by an electromagnetic field of frequency ω. For excitation of a wave of a particular polarization in the sample, it is necessary to orient the field $\mathbf{H}$ appropriately relative to the direction of the electric field in the incident wave. When a weakly damped wave with given polarization is excited in a thin plate with impedance $\zeta(H)$, successive maxima and minima appear, because the resonance relations between the wavelength λ and the plate thickness d are satisfied. Here λ should be comparable in magnitude with d, and, since $d \gg R$, $\lambda = 2\pi/k \gg R$. Thus, long $(kR \ll 1)$ waves are observed experimentally through the oscillations of the impedance of the plate. In this fashion, the spectrum of cyclotron waves in alkali metals has been investigated in detail.[5]

Long-wavelength ordinary waves have been observed in samples of Bi with normal $\mathbf{n} \| C_3$ at $\mathbf{H} \| \mathbf{E} \| C_1$, at a frequency $\omega/2\pi \approx 9.5$ GHz in the range $1 < \Omega/\omega < 2.3$ of interest to us. Subsequent[7] experiments in this geometry were completed on samples of a different thickness. Moreover, the dependence of k on Ω/ω was found in Ref. 7 with the use of an ellipsoidal model of the Fermi surface. In the interval $1.5 < \Omega/\omega < 2.3$, this dependence, expressed as a function of kR on Ω/ω, corresponds to the initial $(kR < 1)$ portion of the spectrum of the ordinary wave in Fig. 1.

As follows from Fig. 1, at $\Omega/\omega < (\Omega/\omega)_0 = 1.45$, the dispersion curve of the ordinary wave becomes a multivalued function of kR. In this connection, we note that an additional series of oscillations of the derivative $d\zeta/dH$, observed on one of the samples of Bi in fields $\Omega/\omega < 1.45$ (Fig. 1 of Ref. 7) evidently results from beating between waves of different k.

In the region $kR \gg 1$, the dividing points of the spectrum in Fig. 1 are the boundary (turning) points, where $d\omega/dk = 0$

and wave propagation ceases. It is natural to assume that, since sharp changes in the structure of the wave take place at these points, then, depending on $\zeta(H)$, features appear in the field H corresponding to the location of the boundaries of the spectrum of cyclotron waves. Thus, for example, in silver,[10] the turning points appear in the form of minima of the signal $d\zeta/dH$. The numerically calculated form of $d\zeta/dH$ as a function of H[10] contains singularities, the location and form of which agree completely with experiment.[10]

In measurements of the surface impedance of bismuth in separate experiments (at frequencies $\sim 10\,\mathrm{GHz}$,[16] Fig. 8 of Ref. 17 and at higher frequencies,[18,19] Fig. 4 from Ref. 20), additional singularities have been observed in the cyclotron resonance region. It is possible that some of these singularities are connected with the excitation of short wavelength cyclotron waves, although detailed investigations of this question were not given in Refs. 16–20. We have attempted to find the short-wavelength boundaries of the spectrum since the method of second harmonic generation is highly sensitive to the bulk properties of Bi under cyclotron resonance conditions.[21]

The Bi sample in the shape of a disk of diameter 17.8 mm with normal $\mathbf{n}\|C_3$ was irradiated by an electromagnetic wave of frequency $d/2\pi = 9.3\,\mathrm{GHz}$. The power of the reflected signal $P_{2\omega}$ at the double frequency 2ω was measured as a function of the external magnetic field $\mathbf{H}\|C_1$, applied parallel to the surface of the sample. The methodology of the experiment is described in detail in Refs. 21 and 22. We only point out that at the frequency ω, the TM_{010} mode is excited in a bimodal cylindrical cavity, the bottom of which is formed by the Bi sample. The lines of force of the electric field of this mode are perpendicular to the surface of the sample, but, because of the finite conductivity of Bi, a transverse component of the electric field appears, having a radial direction and vanishing at the center of the sample. The amplitude of the variable magnetic field reaches the maximum $H_{\sim}$ at the periphery of the sample. Measurements have been carried out on several samples of Bi of thickness between 0.6

and 2 mm.

Figure 3 shows characteristic recordings of the $P_{2\omega}(H)$ signal. Cyclotron resonances are observed in this signal, determined by the condition

$$2\omega = n\Omega, \qquad n = 1,\ 2,\ 3,\dots. \tag{11}$$

Because of the different shape of integer $(n/2 = \text{integer})$ and half-integer resonances,[21] it is more accurate to separate the relation (11) into the condition for observing linear (integer) cyclotron resonances.

$$\omega = n\Omega, \qquad n = 1,\ 2,\ 3,\dots, \tag{12}$$

having the form of maxima of the generated signal $P_{2\omega}$ and the condition for nonlinear (half-integer) resonances

$$\omega = (n - \tfrac{1}{2})\Omega, \qquad n = 1,\ 2,\ 3,\dots, \tag{13}$$

that appear in the form of drops in the radiation.

The values (12) and (13) of the resonance fields of the electrons of ellipsoid (b) are shown in Fig. 3 by the vertical lines. The maximum at 2 is greater than the amplitude of the first resonance, since resonance 1 of the (a) electrons also appears in the field of resonance 2 of the (b) and (c) electrons.

In the doubled magnetic field, the first (b) and (c) resonances and the 1/2 resonance of the (a) electrons appear with different forms. This causes a decrease in the amplitude of resonance 1 and a small shift in the maximum of the signal. We also note that, near the 1 and 3 lines on the highfield side there is an additional structure of the same shape. In all probability the minima indicated with arrows in Fig. 3, which are found in a magnetic field that differs in magnitude by a factor of two, are due to the appearance of cyclotron resonance of the electrons from the vicinity of the reference point.

We now consider the range of magnetic fields $\Omega/\omega > 1$. The positions of the boundaries of the spectrum of longitudinal cyclotron fields are shown by vertical lines and the symbols d_i, corresponding to Fig. 1. As is seen from Fig. 3, the minima in the $p_{2\omega}(H)$ signal correspond to these boundaries. The location of these features does not depend on the thickness of the sample. They had the same form on all the samples investigated. When the temperature increased to $T = 4.2\,\mathrm{K}$, the amplitudes of the minima fell off sharply but their location did not shift with the magnetic field.

The narrow lines $d_7 = (1.64 \pm 0.01)(\Omega/\omega)$ and $d_8 = (1.46 \pm 0.01)(\Omega/\omega)$ were always very clearly seen. As follows from Fig. 1, in the field corresponding to the boundary d_9, several waves are excited with various, but not very different, k. It is possible that such a multiple excitation smoothes out the d_9 singularity. The turning points of the spectrum in the region $1 < \Omega/\omega < d_9$ (Fig. 1) do not appear in the recording of $P_{2\omega}(H)$, since they are found in the immediate vicinity of the first cyclotron resonance. The minima d_6 and especially d_5 are much broader in comparison, for example, with d_7. Thus, in the signal $P_{2\omega}(H)$, the boundaries of the spectrum are found to be isolated in a finite and rather short interval over which the quantity kR varies. The appearance of the longitudinal wave spectrum can be assisted by a strong electric field normal to the surface of the sample. However, it
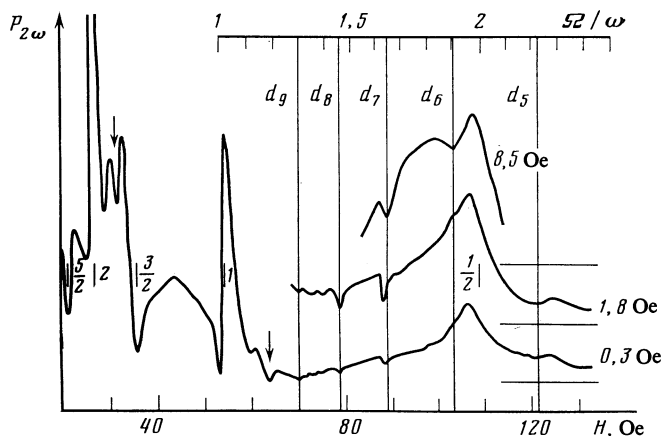
FIG. 3. Recordings of the signal of the second harmonic $P_{2\omega}(H)$ on samples of Bi: $\mathbf{n}\|C_3$, $\mathbf{H}\|C_1$, $\omega/2\pi = 9.3\,\mathrm{GHz}$, $T = 1.5\,\mathrm{K}$. The horizontal lines to the right of the curves indicate the zero levels $P_{2\omega} = 0$ and also the amplitudes of the oscillatory field $H_{\sim}$. The sensitivity on all three curves is different.
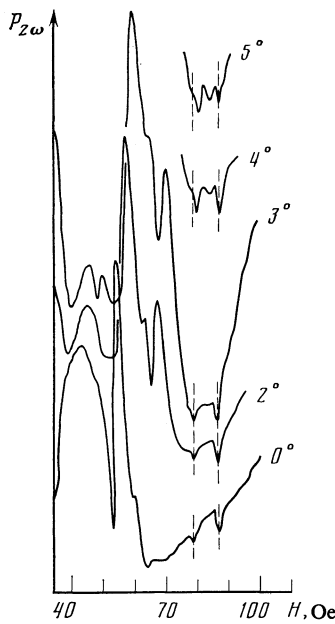
FIG. 4. Small deflections of the magnetic field **H** relative to the C_1 axis in a plane perpendicular to the C_3 axis; $\mathbf{n}\|C_3$, $\omega/2\pi = 9.3$ GHz, $T = 1.5$ K, $H_\sim = 2.3$ Oe.

FIG. 5. Numerical solution of Eq. (1) in the interval between the first and second cyclotron resonances at a frequency of 18.6 GHz; $\mathbf{H}\|C_1$, $\mathbf{k}\|C_3$, $\Omega/\nu \to \infty$.

has not been possible to make clear the wave excitation mechanism in the present experiment.

The location and shape of the peaks did not change when the magnetic field was directed at a small angle from the C_1 axis. In Fig. 4 the minima d_7 and d_8 keep their position for $\chi \lesssim 3°$, where χ is the angle between **H** and C_1. With increasing χ, the left peak shifts in the direction of larger magnetic fields. The value of this shift is much smaller than the shift of the first cyclotron resonance, which by $\chi \approx 6°$ reaches a regime in which the peaks are relocated which leads ultimately to their disappearance.

The increase in the amplitude of the oscillatory field $H_\sim$ from 0.3 to 10 Oe leads only to a small broadening of the observed singularities and in practice has no effect on their shape and location.

Thus, a comparison with the calculation of the spectrum of cyclotron waves in Bi (Fig. 1) enables us to identify the minima (Fig. 3) in the $P_2(H)$ signal as the boundary of the spectrum of longitudinal waves. We note that this comparison was carried out for the frequency $\omega/2\pi = 9.3$ GHz, while the location of the cyclotron resonances was determined by conditions (12) and (13). The relation (11) is equivalent to these two conditions. Therefore, a comparison of the experimentally observed picture with the spectrum of waves at the frequency 2ω is of interest, but in the region of magnetic fields between the first and second cyclotron resonances of the electrons of the (b) ellipsoid. This spectrum, obtained by numerical solution of the general dispersion equation (2), is given in Fig. 5 in the interval $0 < kR < 8$. The approximate expressions (B7) and (B8) and their use in the calculation of Eqs. (8)–(10) allow us to differentiate the different branches of the spectrum in Fig. 5. Thus, the l branch is described by Eq. (10) and is a longitudinal cyclotron wave, squeezed to the left at the line of the first electron cyclotron resonance: the o
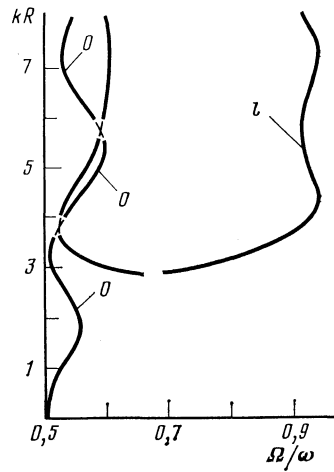
branch corresponds to the solution (8), an ordinary wave, while the other branch, which, just as in the case of curve o, approaches the line of second resonance as kR increases, is described by Eq. (9). It is seen from Fig. 5 that the turning points of the spectrum of cyclotron waves at the doubled frequency 2ω do not correspond to the observed minima in the signal $P_{2\omega}(H)$. The longitudinal waves, propagating in the region $0.5 < \Omega/\omega < 1$ near the hole resonances with numbers $13 \leqslant n \leqslant 24$, exist for $kR > 10$. However, it is clear just from (7) that the boundaries of these waves do not appear in our present experiment.

The author sincerely thanks V. F. Gantmakher, V. Ya. Demikhovskiĭ, E. A. Kaner and G. I. Leviev for useful discussions and interest in the work, and I. D. Zhukovskiĭ for help in carrying out the numerical calculations.

APPENDIX A

We consider the following dependence of the carrier energy on the momentum

$$2\varepsilon = \alpha_{xx}p_x^2 + \alpha_{yy}p_y^2 + \alpha_{zz}p_z^2 + 2\alpha_{xy}p_xp_y + 2\alpha_{xz}p_xp_z + 2\alpha_{yz}p_yp_z. \quad \text{(A1)}$$

Solving the equation of motion in a constant magnetic field

$$\Omega\frac{d\mathbf{p}}{d\varphi} = \frac{e}{c}[\mathbf{vH}],$$

we express the components of the momentum in terms of the variables ε, p and φ:

$$p_x = -m^2 A p_z + \beta(A\cos\varphi - B\sin\varphi),$$
$$p_y = m^2 C p_z - \beta(C\cos\varphi - D\sin\varphi), \quad \text{(A2)}$$

where

$$m = (\alpha_{xx}\alpha_{yy} - \alpha_{xy}^2)^{-1/2},$$
$$A = \alpha_{xy}\alpha_{xz} - \alpha_{yz}\alpha_{xy}, \qquad B = \alpha_{yz}/m,$$
$$C = \alpha_{xy}\alpha_{xz} - \alpha_{xx}\alpha_{yz}, \qquad D = \alpha_{xz}/m,$$
$$\beta = \frac{m}{(A^2 + B^2)^{1/2}}[\alpha_{yy}(2\varepsilon - \gamma p_z^2)]^{1/2},$$
$$\gamma = \alpha_{zz} + m^2(2\alpha_{xz}\alpha_{yz}\alpha_{xy} - \alpha_{xz}^2\alpha_{yy} - \alpha_{yz}^2\alpha_{xx}).$$

From (A1) and (A2), we get the following for the projections of the velocity vector:

$$v_x = \frac{\beta}{m}(D\cos\varphi + C\sin\varphi), \quad v_y = \frac{\beta}{m}(B\cos\varphi + A\sin\varphi), \quad \text{(A3)}$$

$$v_z = \frac{\beta}{\alpha_{yy}}(A^2 + B^2)\cos\varphi + \gamma p_z.$$

We substitute the expressions (A3) in Eqs. (3) and (2), and find the components of the conductivity tensor for any single group of carriers with the dispersion law (A1):

$$\sigma_{xx} = \frac{\alpha_{xy}^2}{\alpha_{yy}}a_1 + \frac{1}{m^2\alpha_{yy}}a_3, \qquad \sigma_{yy} = \alpha_{yy}a_1,$$

$$\sigma_{zz} = \frac{\alpha_{yz}^2}{\alpha_{yy}}a_1 + \frac{A^2 m^2}{\alpha_{yy}}a_3 + \gamma a_4,$$

$$\sigma_{xy} = \alpha_{xy}a_1 - ia_2/m, \qquad \sigma_{yx} = \sigma_{xy}^*, \qquad \text{(A4)}$$

$$\sigma_{yz} = \alpha_{yz}a_1 + iAma_2, \qquad \sigma_{zy} = \sigma_{yz}^*,$$

$$\sigma_{xz} = \frac{\alpha_{xy}\alpha_{yz}}{\alpha_{yy}}a_1 + iCma_2 + \frac{A}{\alpha_{yy}}a_3, \qquad \sigma_{zx} = \sigma_{xz}^*,$$

where

$$a_1 = \frac{N}{(kR)^2}\sum_n \frac{n^2}{\nu - i(\omega - n\Omega)}\int_0^{\pi/2} d\theta \sin\theta J_n^2(kR\sin\theta),$$

$$a_2 = \frac{N}{kR}\sum_n \frac{n}{\nu - i(\omega - n\Omega)}$$
$$\times \int_0^{\pi/2} d\theta \sin^2\theta J_n(kR\sin\theta)J_n'(kR\sin\theta),$$

$$a_3 = N\sum_n \frac{1}{\nu - i(\omega - n\Omega)}\int_0^{\pi/2} d\theta \sin^3\theta J_n'^2(kR\sin\theta), \qquad \text{(A5)}$$

$$a_4 = N\sum_n \frac{1}{\nu - i(\omega - n\Omega)}\int_0^{\pi/2} d\theta \sin\theta\cos^2\theta J_n^2(kR\sin\theta),$$

$$N = \frac{(2\varepsilon)^{1/2}me^2}{\pi^2\hbar^3\gamma^{1/2}}, \quad R = \frac{(2\varepsilon\alpha_{yy})^{1/2}}{\Omega} = \frac{mc}{eH}(2\varepsilon\alpha_{yy})^{1/2}.$$

Here we have introduced the variable $\theta = \arccos[(\gamma/2\varepsilon)^{1/2}p_z]$, and J_n and J_n' and the Bessel function of order n and its derivative with respect to its argument.

APPENDIX B

We not obtain the asymptotic expressions for the elements of the tensor σ_{ij} in the limit $kR \gg 1$, basing the calculation of the components of the susceptibility tensor of a degenerate Fermi gas on the treatment given in Ref. 4.

We introduce the designations $kR = x$, $\omega/\Omega = y$ for the electrons of ellipsoid (b) and write the quantities a_i from (A5) as $\nu \to 0$ in a form convenient for calculations in the limiting case $x \gg 1$. Using the addition theorem for Bessel functions[23] and the relation

$$\frac{1}{y-n} = \frac{1}{i}\int_0^\infty e^{-i(y-n)t}\,dt,$$

we obtain

$$a_1 = -\frac{iNy^2}{\omega x^2}\left[1 + 2iy\int_0^{\pi/2} d\theta \sin\theta \int_0^\infty dt e^{2iyt}J_0(2x\sin\theta\sin t)\right],$$

$$a_2 = -\frac{2Ny^2}{\omega x}\int_0^{\pi/2} d\theta \sin^2\theta \int_0^\infty dt e^{2iyt}\sin t J_1(2x\sin\theta\sin t), \quad \text{(B1)}$$

$$a_3 = \frac{2Ny}{\omega}\int_0^{\pi/2} d\theta \sin^3\theta \int_0^\infty dt e^{2iyt}\cos 2t J_0(2x\sin\theta\sin t) - a_1,$$

$$a_4 = \frac{2Ny}{\omega}\int_0^{\pi/2} d\theta \sin\theta\cos^2\theta \int_0^\infty dt e^{2iyt}J_0(2x\sin\theta\sin t).$$

At $x \gg 1$, the basic contribution to the integrals in the variable t is made by values of t close to $t_m \approx m\pi (m = 0,1,2,\ldots)$. Calculation of the quantities a_i from (B1) reduces to finding the sum

$$\sum_{m=0}^\infty \int_0^\infty dt e^{2iyt_m}J_0(2x\sin\theta\sin t_m) = \begin{cases} \dfrac{i\,\text{ctg}\,\pi y}{2(x^2\sin^2\theta - y^2)^{1/2}} & (y < x\sin\theta) \\[6pt] \backslash \\[6pt] \dfrac{i}{2(y^2 - x^2\sin^2\theta)^{1/2}} & (y > x\sin\theta) \end{cases} \qquad \text{(B2)}$$

The a_i thus obtained determine the chief terms in the expansion of the components of σ_{ij} from (A4) in powers of $1/x$, but do not contain terms oscillating in x, which are responsible for oscillations of the spectrum in Fig. 1. To find the correction components to the expressions for a_i we use the relations[23,24]

$$J_n^2(z) = \frac{1}{\pi}\int_0^\pi J_0(2z\sin\varphi)\cos 2n\varphi\,d\varphi, \qquad J_{\mu+1}(z) = \frac{z^{\mu+1}}{2^\mu\Gamma(\mu+1)}\int_0^{\pi/2} J_0(z\sin\varphi)\sin\varphi\cos^{2\mu+1}\varphi\,d\varphi,$$

$$\left(\frac{\pi}{2z}\right)^{1/2}J_{n+1}(z) = \frac{z^n}{2^{n+1}n!}\int_0^\pi \cos(z\cos\psi)\sin^{2n+1}\psi\,d\psi, \qquad J_{2n}(z) = \frac{1}{\pi}\int_0^\pi \cos(z\sin\psi)\cos 2n\psi\,d\psi \qquad \text{(B3)}$$

and rewrite (A5) in the form

$$a_1 = \frac{iNy^2}{\omega x^2}\left[\, y \sum_n \frac{I_1(n,x)}{y-n} - 1 \right],$$

$$a_3 = \frac{iNy}{4\omega} \sum_n \frac{I_1(n+1,x)+I_2(n+1,x)+I_1(n-1,x)+I_2(n-1,x)}{y-n},$$

$$a_4 = \frac{iNy}{\omega} \sum_n \frac{I_1(n,x)-I_2(n,x)}{y-n}, \tag{B4}$$

where

$$I_1(n,x) = \int_0^1 J_{2n}(2xu)\,du, \qquad I_2(n,x) = \int_0^1 J_{2n}(2xu)\,u^2\,du.$$

Since

$$\cos(z\sin\theta) = \sum_{n=-\infty}^{\infty} J_{2n}(z)\exp(-2in\theta),$$

while from the second formula of (B3) we have

$$\int_0^{\pi/2} J_1(2x\sin\theta\sin t)\sin^2\theta\,d\theta = \frac{1}{2x\sin t}\left[\int_0^{\pi/2} J_0(2x\sin\theta\sin t)\right.$$
$$\left. \times \sin\theta\,d\theta - \cos(2x\sin t)\right],$$

we obtain the following immediately from (B1) and (B4):

$$a_2 = \frac{iNy^2}{2\omega x^2} \sum_n \frac{J_{2n}(2x)-I_1(n,x)}{y-n}. \tag{B5}$$

The integrals $I_1(n,x)$ and $I_2(n,x)$ are expressed in terms of the Lommel functions $S_{\mu,\nu}(z)^{24}$ with the help of the formula

$$\int_0^z z^\mu J_\nu(z)\,dz = (\mu+\nu-1)zJ_\nu(z)S_{\mu-1,\nu-1}(z) - zJ_{\nu-1}(z)S_{\mu,\nu}(z). \tag{B6}$$

The Lommel functions for $z \gg 1$ have the asymptote $S_{\mu,\nu}(z) \approx z^{\mu-1}$. The oscillations of the dispersion curve in the case of large x are due to the oscillatory dependence on x of the principal term of the asymptotic expansion of the function $J_{2n}(2x)$.

We determine the oscillating correction to the expressions for a_i, [which latter are obtained by substitution of (B2) in (B1)] by use of (B4) and (B5), and with the help of (B6) and the relation

$$\sum_n \frac{(-1)^n}{y-n} = \pi\,\mathrm{cosec}\,\pi y.$$

As a result of summation in the case $x > y$, we obtain

$$a_1 = -\frac{iNy^2}{\omega x^2}\left[1 - \frac{y}{2x}\left(\pi\,\mathrm{ctg}\,\pi y + \ln\frac{x+y}{x-y}\right) + \frac{y}{2x} \right.$$
$$\left. \times \left(\frac{\pi}{2x}\right)^{1/2} (\cos 2x - \sin 2x)\,\mathrm{cosec}\,\pi y \right],$$

$$a_2 = \frac{iNy^2}{2\omega x^2}\left[-\frac{1}{2x}\left(\pi\,\mathrm{ctg}\,\pi y + \ln\frac{x+y}{x-y}\right) \right.$$
$$\left. + \left(\frac{\pi}{2x}\right)^{1/2} (\cos 2x + \sin 2x)\,\mathrm{cosec}\,\pi y \right],$$

$$a_3 = \frac{iNy}{2\omega x}\left[\frac{y}{x} + \frac{1}{2}\left(\pi\,\mathrm{ctg}\,\pi y + \ln\frac{x+y}{x-y}\right)\left(1 - \frac{y^2}{x^2}\right) \right.$$
$$\left. + \left(\frac{\pi}{2x}\right)^{1/2} (\cos 2x - \sin 2x)\,\mathrm{cosec}\,\pi y \right],$$

$$a_4 = \frac{iNy}{2\omega x}\left[\frac{y}{x} + \frac{1}{2}\left(\pi\,\mathrm{ctg}\,\pi y + \ln\frac{x+y}{x-y}\right)\left(1 - \frac{y^2}{x^2}\right) \right.$$
$$\left. - \frac{1}{2x}\left(\frac{\pi}{2x}\right)^{1/2} (\cos 2x + \sin 2x)\,\mathrm{cosec}\,\pi y \right], \tag{B7}$$

while at $x < y$,

$$a_1 = -\frac{iNy^2}{\omega x^2}\left(1 - \frac{y}{2x}\ln\frac{y+x}{y-x}\right), \qquad a_2 = -\frac{iNy^2}{2\omega x^3}\ln\frac{y+x}{y-x},$$

$$a_3 = a_4 = \frac{iNy}{2\omega x}\left[\frac{y}{x} + \frac{1}{2}\ln\frac{y+x}{y-x}\left(1 - \frac{y^2}{x^2}\right) \right]. \tag{B8}$$

As in seen from (B7) and (B8), the period Δx of the oscillations of the functions $a_i(x)$ is given by $\Delta x = \pi$, while the amplitude of the oscillations falls off with increase in x.

The expressions (B7) and (B8) were obtained for the electrons of the (b) and (c) ellipsoids. Taking into account the change in the quantities N, x, y, similar relations can be written down for the electrons of the ellipsoid (a) and for the holes. Summing the contributions from all the carriers in (B7) and (B8) and substituting a_i in (A4), we obtain the elements of the tensor σ_{ij}. If we include terms up to $x^{-3/2}$ in the components σ_{xx} and σ_{zz}, then at $x \gg 1$, the dispersion equation (1) decomposes into Eqs. (8), (9) and (10).

[1]E. A. Kaner and V. G. Skobov, Fiz. Tverd. Tela 6, 1104 (1964); [Sov. Phys. Solid State 6, 851 (1964)].
[2]W. M. Walsh and P. M. Platzman, Phys. Rev. Lett. 15, 784 (1965).
[3]E-Ni Foo, Phys. Rev. 182, 674 (1969).
[4]T. D. Kaladze, D. G. Lominadze and K. N. Stepanov, Fiz. Tverd. Tela 11, 3312 (1973); [Sov. Phys. Solid State 11, 2681 (1973)].
[5]F. Platzman and P. Vol'f, Volny i vzaideistviya v plazme tverdogo tela (Waves and Interactions in Solid State Plasma) Mir, Moscow, 1975.
[6]V. S. Edel'man and M. S. Khaĭkin, Zh. Eksp. Teor. Fiz. 45, 826 (1963); [Sov. Phys. JETP. 18, 566 (1964)].
[7]V. S. Edel'man, Pis'ma Zh. Eksp. Teor. Fiz. 9, 302 (1969); [JETP Lett. 9, 177 (1969)].

1093   Sov. Phys. JETP 61 (5), May 1985

M. R. Trunin   1093

[8]V. P. Naberezhnykh, D. E. Zherebchevskii, A. N. Poluyanenko, A. V. Vetchinov and N. K. Dan'shin, Fiz. Nizhn. Temp. **2**, 1144 (1976); [Sov. J. Low Temp. Phys. **2**, 359 (1976)].

[9]V. P. Naberezhnykh, D. E. Zherebchevskii and V. L. Mel'nik, Pis'ma Zh. Eksp. Teor. Fiz. **13**, 150 (1971); [JETP Lett. **13**, 150 (1972)]; Zh. Eksp. Teor. Fiz. **63**, 169 (1972); [Sov. Phys. JETP **36**, 89 (1973)].

[10]J. O. Henningsen, J. Low Temp. Phys. **4**, 163 (1971).

[11]G. L. Danifer, P. H. Schmidt and W. M. Walsh, Phys. Rev. Lett. **26**, 1553 (1971).

[12]E. A. Kaner and V. G. Skobov, Adv. Phys. **17**, 605 (1968).

[13]A. P. Korolyuk, Zh. Eksp. Teor. Fiz. **49**, 1009 (1965); [Sov. Phys. JETP **22**, 701 (1966)].

[14]V. S. Edel'man, Usp. Fiz. Nauk, **102**, 55 (1970); [Sov. Phys. Uspekhi, **13**, 583 (1971)].

[15]A. B. Pippard, Phil. Mag. **2**, 1147 (1957).

[16]V. S. Edel'man, Zh. Eksp. Teor. Fiz. **83**, 2317 (1982); [Sov. Phys. JETP **56**, 1343 (1982)].

[17]V. S. Edel'man, Usp. Fiz. Nauk **123**, 257 (1977); [Sov. Phys. Uspekhi **20**, 819 (1977).

[18]W. Braune, J. Lebech and K. Saermark, Sol. State Commun. **26**, 13 (1978).

[19]G. E. Smith, L. C. Hebel and S. J. Buchsbaum, Phys. Rev. **129**, 154 (1963).

[20]U. Strom, A. Kamgar and J. F. Koch, Phys. Rev. **7**, 2435 (1973).

[21]V. F. Gantmakher, G. N. Leviev and M. R. Trunin, Zh. Eksp. Teor. Fiz. **82**, 1607 (1982); [Sov. Phys. JETP **55**, 931 (1982)].

[22]V. F. Gantmakher, G. N. Leviev and M. R. Trunin, Zh. Eksp. Teor. Fiz. **85**, 1489 (1963); [Sov. Phys. JETP **58**, 863 (1983)].

[23]M. Abramovich and I. Stegun, Handbook of Mathematical Functions, Dover Publication, NY, 1972.

[24]G. N. Watson, A Treatise on the Theory of Bessel Functions, 2nd ed., Cambridge University Press, 1966.

Translated by R. T. Beyer

1094   Sov. Phys. JETP **61** (5), May 1985

M. R. Trunin   1094